

Transmission properties of surface plasmon polaritons and localized resonance in semiconductor hole arrays

T. Okada,^{1,a)} S. Tsuji,² K. Tanaka,² K. Hirao,² and K. Tanaka³

¹*Pioneering Research Unit for Next Generation, Kyoto University, Kyoto 615-8245, Japan*

²*Department of Material Chemistry, Graduate School of Engineering, Kyoto University, Kyoto 615-8510, Japan*

³*Institute for Integrated Cell-Material Sciences, Kyoto University, Kyoto 606-8502, Japan*

(Received 3 August 2010; accepted 22 November 2010; published online 29 December 2010)

We study optical modulated transmission in semiconductor hole arrays using terahertz time-domain measurements in combination with the optical pump-terahertz probe technique. When the density of photoexcited carriers is varied, we observe an evanescent decay profile for the propagation of surface plasmon polaritons, whereas steady behavior is exhibited for transmission attributed to the localized resonance in the holes. We also demonstrate an optically controlled transition of the transmission mechanism, attributed to the change from a dielectric structure to a plasmonic material. © 2010 American Institute of Physics. [doi:10.1063/1.3532111]

The remarkable finding of resonant optical transmission through hole arrays (HAs) in metallic films where the holes are of subwavelength dimensions¹ has generated much attention in recent years. The mechanism of transmission in periodic metal HAs has become the focus of investigation with a view to realizing subwavelength photodevices, plasmonic devices that operate beyond the diffraction limit.² It is generally believed that the dominant mechanism causing resonant transmission involves the excitation of surface plasmon polaritons (SPPs) at the metal-dielectric interface.^{3–5} Studies on arrays of rectangular holes have revealed that the local resonance (LR) can also mediate transmission; the dominant mechanism can be changed continuously by controlling the length ratio of the long and short sides of the rectangular holes.^{4,6,7}

The terahertz frequency regime, which is commonly defined as the region of the electromagnetic spectrum between 0.3 and 10 THz, is attractive for a variety of applications in science and technology such as sensing, imaging, and telecommunication. In this frequency region, the use of metallic structures is essential because metals are nearly perfect conductors. In practice, semiconductor HAs with high densities of doped carriers are more suitable because they conduct as metals^{8,9} and potentially allow real-time operation of the terahertz transmission. The permittivity of such semiconductors can be controlled by thermal modulation¹⁰ or photo-injected free carriers,^{9,11} which implies that optical switching of terahertz pulses is possible. In the latter case, the use of time-domain (TD) spectroscopy to probe the inhomogeneous photoinduced carrier distribution has confirmed that the carrier layer is metallic.¹²

Here, we investigate the influence of the carrier distribution on the transmission properties of semiconductor HAs, considering both the excitation of SPPs and the LR in the holes. By combining terahertz-TD spectroscopy with the optical pump-terahertz probe technique, we reveal an evanescent decay profile with increasing photocarrier density for the propagation of SPPs and steady behavior for the LR in the holes. We also discuss the influence of the plasma fre-

quency of the back interface on the appearance of the characteristic resonant transmission.

Semiconductor HAs were constructed from high-resistivity Si ($R > 1000 \Omega \text{ cm}$), for which the refractive index is $\epsilon_{\text{Si}}^{1/2} = 3.4$ in the terahertz frequency regime. Si wafers of thickness $h = 50 \mu\text{m}$ were perforated periodically with circular holes arranged in a hexagonal lattice structure. We prepared two samples; the lattice constant and hole diameters of $a = 750 \mu\text{m}$ and $d = 300 \mu\text{m}$ and $a = 300 \mu\text{m}$ and $d = 150 \mu\text{m}$, respectively. Our experimental setup consisted of a terahertz-TD measurement system incorporating the optical pump-terahertz probe technique, details of which are described in a previous paper.¹² One interface of the Si wafer was irradiated by the optical pump pulse, and the terahertz probe pulse was transmitted perpendicular to this interface. The optical pump power P was varied up to 100 mW, at which the corresponding carrier density at the front (irradiated) interface of the Si wafer is $4.2 \times 10^{18} \text{ cm}^{-3}$ and the plasma frequency is 13.4 THz. The timing of the terahertz pulse was set to 5 ps after the arrival of the optical pump pulse at the Si interface; this time delay is large compared to the rise time of the photoinduced structure,¹³ and sufficiently shorter than the relaxation time and diffusion time $D_p^2/4D \approx 100 \text{ ns}$, where $D_p = 12.2 \mu\text{m}$ and D are the skin depth of Si at a wavelength of 800 nm,^{14,15} and the self-diffusion coefficient of photoexcited carriers,¹⁶ respectively. We can therefore assume that the photocarriers in our study possess free-carrier properties.¹⁷

Figure 1 shows the evolution of the transmission spectra with optical pump power for the Si HA with $a = 750 \mu\text{m}$ and $d = 300 \mu\text{m}$. The transmission is dominated by Fabry-Pérot oscillations except in the low-frequency region at zero optical pump power, as shown in the inset. The frequency of the spectral minimum can be expressed as $f_{\text{FP}} = c(m + 1/2) \times (2h\epsilon_{\text{Si}}^{1/2})^{-1}$, where c is the velocity of light in vacuum and m is an integer; this gives zeroth, first, and second order interferences of 0.44, 1.32, and 2.21 THz, respectively. On optical excitation, the transmittance in the higher frequency regime abruptly decreases due to conductivity losses, and the Fabry-Pérot interference pattern is diminished. Furthermore, a characteristic transmission peak appears at $\sim 0.4 \text{ THz}$, which can be attributed to the SPP resonance through the

^{a)}Author to whom correspondence should be addressed. Electronic mail: t.okada@kupra.iae.kyoto-u.ac.jp.

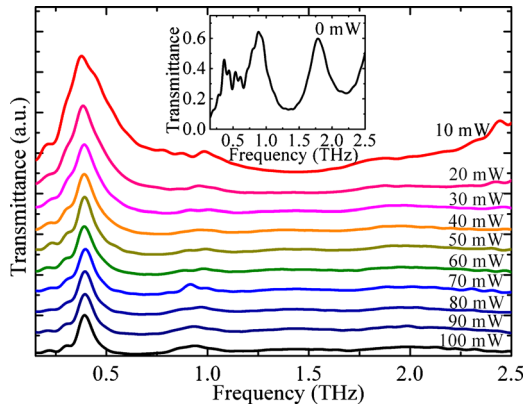


FIG. 1. (Color online) Transmission spectra in the frequency domain through a subwavelength HA with period $750 \mu\text{m}$ and hole diameter $300 \mu\text{m}$, at different values of optical pump power. The transmission in the absence of a sample was employed as a reference spectrum. The spectra have been offset vertically for clarity. The inset shows the transmission spectrum under zero excitation.

HA. The frequency of the SPP mode at normal terahertz incidence is approximately given by $f_{\text{SW}} = c(\epsilon_d + \epsilon_{\text{Si}})^{1/2} / a(\epsilon_d \epsilon_{\text{Si}})^{1/2}$, where $\epsilon_d = \epsilon_{\text{air}} = 1$ is the vacuum permittivity.⁸ We calculate the SPP frequency under the assumption that $|\epsilon_{\text{Si}}| \gg \epsilon_d$ because the plasma frequency is much larger than the transmission peak frequency. In the irradiated region of the Si wafer, the density of photoexcited carriers and the corresponding plasma frequency exponentially decrease with depth perpendicular to the wafer surface.^{12,17} When the optical pump power is increased to 10 mW, at which the transmission peak already appears, the plasma frequencies at the front and back interfaces are 4.2 and 0.55 THz, respectively. We note that with an increasing optical pump power, the transmission peak frequency is slightly blue-shifted from 0.38 to 0.4 THz, which is consistent with a previous report.¹¹ This observation can be explained by the modified real part of the permittivity of Si in accordance with $\epsilon_{\text{Si}}(1 - f_{\text{pl}}^2/f^2)$, together with the Drude model, where f_{pl} is the plasma frequency of photoexcited Si. This peak is calculated to appear at 0.38 THz when $f_{\text{pl}} \approx 0.52$ THz. We also note that the peak appears below the cut-off frequency predicted by the circular metallic waveguide theory. This indicates that in the holes, light becomes an evanescent mode rather than a propagation mode.

The characteristic resonant transmission can be attributed to the coupling mode between the SPPs and LR; for rectangular holes, the dominant mechanism can be changed from the excitation of SPPs to the LR by tuning the length ratio of the long and short sides.^{4,6,7} Characteristic transmission attributed mainly to the LR has also been observed for square and circular holes.⁶ Figure 2 shows the evolution of transmission spectra with optical pump power for the HA with $a = 300 \mu\text{m}$ and $d = 150 \mu\text{m}$. At zero optical excitation, as shown in the inset, the Fabry-Pérot interference is observed at a higher frequency than that estimated. This implies that the refractive index of Si is decreased in the effective medium theory when the percentage hole occupancy η (defined as the ratio of the hole area to the total surface area) is large. In addition, the transmission is dominated by other complex features due to guided resonances, namely, the effect of the photonic crystal.^{9,10,18} The photonic crystal effect tends to appear as the value of η increases; thus, it is not observed in Fig. 1 ($\eta = 14.5\%$), but is apparent in Fig. 2

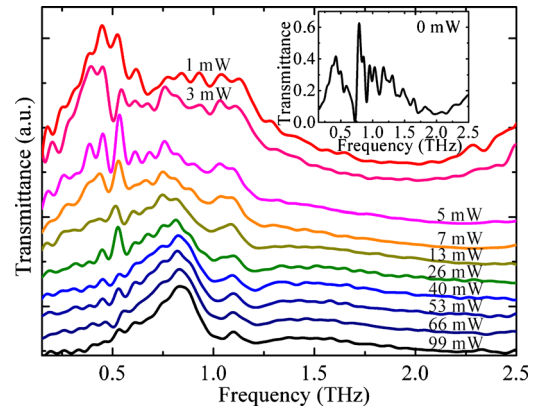


FIG. 2. (Color online) Transmission spectra in the frequency domain through a subwavelength HA with period $300 \mu\text{m}$ and hole diameter $150 \mu\text{m}$, at different values of optical excitation power. The transmission in the absence of a sample was employed as a reference spectrum. The spectra have been offset vertically for clarity. The inset shows the transmission spectrum under zero excitation.

($\eta = 23\%$). We note that the photonic crystal effect was not observed in the transmission spectrum of a Si HA with $d = 200 \mu\text{m}$ and $a = 750 \mu\text{m}$ ($\eta = 6.4\%$), whereas it was apparent in the spectrum of a HA with $d = 300 \mu\text{m}$ and $a = 500 \mu\text{m}$ ($\eta = 33\%$), in both cases without optical excitation (data not shown). On optical excitation, the photonic crystal effect in HAs with larger η abruptly disappears, as shown in Fig. 2. Simultaneously, a broad transmission peak appears at 0.83 THz, the asymmetrical profile of which is likely due to Fano resonance.⁹ The frequency of this peak is slightly lower than that estimated assuming the SPP or LR mechanisms (1 THz). It is probable that the actual hole diameter is slightly larger than the nominal diameter due to the finite penetration depth of terahertz waves at the poorly metallic hole walls.¹² Moreover, we can assume that the diffusion and recombination of photoexcited carriers are negligible in our experiment.^{12,14-17} Therefore, the carrier density at the hole walls decays exponentially with increasing depth, causing a red-shift of the transmission peak due to the LR. We thus assume that the transmission peak for the HA with $d = 150 \mu\text{m}$ and $a = 300 \mu\text{m}$ can mainly be attributed to the LR. We also note that the plasma frequency of photoexcited Si is assumed to be much higher than the transmission peak frequency (for $P > 26$ mW), which implies that $|\epsilon_{\text{Si}}| \gg \epsilon_d$. This does not hold in the low pump power regime; thus the frequency of the transmission peak would deviate from the theoretical value; however, the peak position is rather poorly defined in our study. It is also noteworthy that the peak becomes much more pronounced at pump powers greater than 26 mW, for which the corresponding plasma frequency at the back interface of the Si wafer is 0.88 THz. Therefore, we suggest that the transmission peak clearly emerges when the plasma frequency at the back interface exceeds the transmission peak frequency.

The inhomogeneous distribution of carriers as a function of the depth in the Si wafer has a significant influence on the intensity of the transmission peaks. Figure 3 shows the transmission efficiency, defined as the transmittance at the peak frequency normalized by the surface area occupied by the holes, as a function of the optical pump power. The transmission efficiency for the HA with $d = 300 \mu\text{m}$ and $a = 750 \mu\text{m}$ gradually decreases with increasing pump power, whereas essentially steady behavior is exhibited for the HA

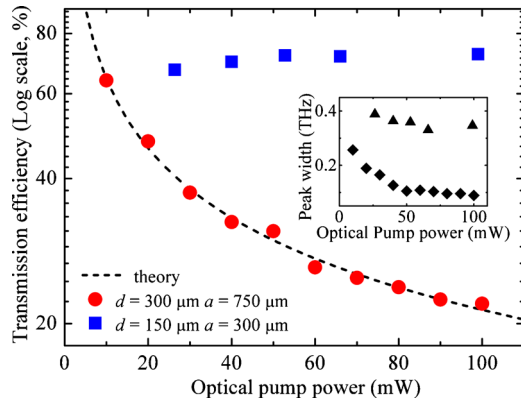


FIG. 3. (Color online) Transmission efficiency of two samples at the peak frequency as a function of optical pump power. The inset shows the dependence of peak width on optical pump power for Si HAs with $d=300 \mu\text{m}$, $a=750 \mu\text{m}$ (diamonds) and with $d=150 \mu\text{m}$, $a=300 \mu\text{m}$ (triangles).

with $d=150 \mu\text{m}$ and $a=300 \mu\text{m}$. These trends can also be observed in the peak widths shown in the inset. In order to investigate the nonpropagating nature of the SPPs, we evaluated the decay profile of the transmission peak intensity in the former case. We assume that in a Si wafer with a HA, the transmission efficiency for the SPP mode exponentially decreases with thickness, with a characteristic decay length L_c .⁸ The transmission efficiency is expressed as

$$T_{\text{eff}}(N_{\text{pump}}) \propto \left(\frac{N_{\text{pump}} e^2}{4\pi S D_p \mu \epsilon_{\text{Si}} \epsilon_0 f_p^2} \right)^{-h/L_c}, \quad (1)$$

where $1/\mu = 1/m_e + 1/m_h$ is a function of the reduced masses of the electron and the hole [m_e and m_h are the effective masses of electrons and holes in Si (Ref. 19)], N_{pump} (2.7×10^{12}) is the optical pump photon number per pulse, S ($9^2 \pi \text{mm}^2$) is the irradiated area, ϵ_0 is the permittivity of free space, and e is the electron charge. In this calculation, we assume that the carrier plasma is in equilibrium, that the number of photoexcited electrons and holes is equal to the optical pump photon number, and that $f_p^2 = f_{pe}^2 + f_{ph}^2$. As shown in Fig. 3, the theoretical curve obtained for a plasma frequency of $f_p = 0.4 \text{ THz}$ is in good agreement with the experimental curve when $L_c = 25.5 \mu\text{m}$. The characteristic decay length for the HA with $d=200 \mu\text{m}$ and $a=750 \mu\text{m}$ ($\eta = 6.4\%$) was obtained in similar fashion and found to be $L_c = 20.8 \mu\text{m}$. These values of L_c are slightly smaller than in doped semiconductors,⁸ which is due to the inhomogeneous carrier distribution. By contrast, the LR exhibits a profile that does not decay with increasing pump power, implying that the localized electromagnetic wave inside the holes does not propagate from the front to the back interface.

Here, we remark that published experimental data for the visible and near-infrared regimes suggest that no resonant feature is present in the transmission spectrum for circular HAs.^{20,21} By contrast, transmission due to the LR can be observed for a single circular hole in the terahertz regime because the penetration depth is extremely shallow compared to the incident wavelength, although the enhancement factor should be small.^{3,6} Finally, we note that another possible explanation can be examined to account for the lower frequency of the transmission peak in Fig. 2 than that estimated for the SPP. At large values of η , the SPP can be regarded as a spoof SPP when the metal-vacuum effective medium

model is considered. This implies that the position of the corresponding transmission peak is shifted to lower frequency because the nominal penetration depth would increase and the velocity would decrease for a SPP with spoof characteristics. In a photoexcited system the penetration depth and velocity should depend on the carrier density, which implies that the position and intensity of the transmission peak should vary with pump power. However, we do not observe such a tendency in our experiment.

In conclusion, we have measured the transmission properties of a photodoped semiconductor mediated both by the excitation of SPPs and by the LR. A transmission peak clearly emerges when the plasma frequency of the back interface exceeds the transmission peak frequency. The transmission efficiency decays with increasing optical pump power for the excitation of SPPs, whereas no dependence on the optical carrier density is observed for the LR. Furthermore, we have demonstrated a continuous transition from a dielectric structure to a plasmonic material. This study will contribute to the realization of all-optical operating devices such as optical integrated circuits, as well as basic optical components. To improve the switching speed, a more suitable semiconductor could be chosen, for example, a direct semiconductor such as GaAs, InSb, or InAs.

This study is supported by the Special Coordination Funds for Promoting Science and Technology, and by the Grant-in-Aid for Scientific Research (Grant No. 20104007) commissioned by the MEXT of Japan. This work is also supported by the Murata Science Foundation.

¹T. W. Ebbesen, L. J. Lezec, H. F. Ghaemi, T. Thio, and P. A. Wolff, *Nature (London)* **391**, 667 (1998).

²S. A. Maier, *Plasmonics: Fundamentals and Applications* (Springer, New York, 2007).

³F. Miyamaru and M. Hangyo, *Appl. Phys. Lett.* **84**, 2742 (2004).

⁴J. Han, A. K. Azad, M. Gong, X. Lu, and W. Zhang, *Appl. Phys. Lett.* **91**, 071122 (2007).

⁵J. Braun, B. Gompf, G. Kobiela, and M. Dressel, *Phys. Rev. Lett.* **103**, 203901 (2009).

⁶F. J. García-Vidal, E. Moreno, J. A. Porto, and L. Martín-Moreno, *Phys. Rev. Lett.* **95**, 103901 (2005).

⁷F. Miyamaru and M. W. Takeda, *Phys. Rev. B* **79**, 153405 (2009).

⁸C. Janke, J. Gómez Rivas, C. Schotsch, L. Beckmann, P. Haring Bolivar, and H. Kurz, *Phys. Rev. B* **69**, 205314 (2004).

⁹W. Zhang, A. K. Azad, and J. Han, *Phys. Rev. Lett.* **98**, 183901 (2007).

¹⁰J. Gómez Rivas, M. Kuttge, H. Kurz, P. Haring Bolivar, and J. A. Sánchez-Gil, *Appl. Phys. Lett.* **88**, 082106 (2006).

¹¹C. Janke, J. Gómez Rivas, P. Haring Bolivar, and H. Kurz, *Opt. Lett.* **30**, 2357 (2005).

¹²T. Okada, K. Ooi, Y. Nakata, K. Fujita, K. Tanaka, and K. Tanaka, *Opt. Lett.* **35**, 1719 (2010).

¹³R. Huber, F. Tauser, A. Brodschelm, M. Bichler, G. Abstreiter, and A. Leitenstorfer, *Nature (London)* **414**, 286 (2001).

¹⁴E. D. Palik, *Handbook of Optical Constants of Solids III* (Academic, Boston, MA, 1998).

¹⁵E. Yablonovitch, D. L. Allara, C. C. Chang, T. Gmitter, and T. B. Bright, *Phys. Rev. Lett.* **57**, 249 (1986).

¹⁶C. M. Li, T. Sjödin, and H. L. Dai, *Phys. Rev. B* **56**, 15252 (1997).

¹⁷M. C. Beard, G. M. Turner, and C. A. Schmuttenmaer, *Phys. Rev. B* **62**, 15764 (2000).

¹⁸Z. Jian and D. M. Mittleman, *Appl. Phys. Lett.* **87**, 191113 (2005).

¹⁹D. M. Riffe, *J. Opt. Soc. Am. B* **19**, 1092 (2002).

²⁰T. Thio, H. F. Ghaemi, H. J. Lezec, P. A. Wolff, and T. W. Ebbesen, *J. Opt. Soc. Am. B* **16**, 1743 (1999).

²¹K. J. K. Koerkamp, S. Enoch, F. B. Segerink, N. F. van Hulst, and L. Kuipers, *Phys. Rev. Lett.* **92**, 183901 (2004).